Journal of Theoretical Biology 468 (2019) 60–71

Contents lists available at ScienceDirect

Journal of Theoretical Biology

journal homepage: www.elsevier.com/locate/jtb

# Phytoplankton adaptation in ecosystem models

Aike Beckmann[a], C-Elisa Schaum[b], Inga Hense[c,*]

[a] AIONATEM, Hamburg, Germany
[b] IMF, CEN, Universität Hamburg, Olbersweg 24, Germany
[c] IMF, CEN, Universität Hamburg, Grosse Elbstrasse 133, Germany

ARTICLE INFO

*Article history:*
Received 27 September 2018
Revised 3 December 2018
Accepted 21 January 2019
Available online 20 February 2019

*Keywords:*
Thermal adaptation
Individual based model (IBM)
Multi-compartment model (MCM)
Trait diffusion model
NPZD-Type model
Adaptive evolution

ABSTRACT

We compare two different approaches to model adaptation of phytoplankton through trait value changes. Both consider mutation and selection (MuSe) but differ with respect to the underlying conceptual framework. The first one (MuSe-IBM) explicitly considers a population of individuals that are subject to random mutation during cell division. The second is a deterministic multi-compartment model (MuSe-MCM) that considers numerous genotypes of the population and where mutations are treated as a transfer of biomass between neighboring genotypes (i.e., a diffusion of characteristics in trait space). Focusing on the adaptation of optimal temperature, we show model results for different scenarios: a sudden change in environmental temperature, a seasonal variation and high frequency fluctuations. In addition, we investigate the effect of different shapes of thermal reaction norms as well as the role of alternating growth and resting phases on the adaptation process. For all cases, the differences between MuSe-IBM and MuSe-MCM are found to be negligible. Both models produce a number of well-known and plausible features. While the IBM has the advantage of including more mechanistic (i.e., probabilistic) processes, the MCM is much less computationally demanding and therefore suitable for implementation in three-dimensional ecosystem models.



## 1. Introduction

The adaptation potential of phytoplankton populations has received more and more attention over the past years (e.g. O'Donnell et al., 2018; Lohbeck et al., 2012; Schaum et al., 2017). As adaptation to environmental changes is observed to take place on time scales similar to the ecological ones – "rapid adaptation" (sensu Hairston et al., 2005) – this process needs to be included in aquatic ecosystem and biogeochemical models. Several different approaches to account for adaptation through trait value changes have been proposed, including an individual based (e.g. Clark et al., 2011) and a compartment based, the so-called "trait diffusion", approach (e.g. Kremer and Klausmeier, 2013). We compare these two fundamentally different ways to test the effects of mutation and selection in phytoplankton populations by investigating a number of idealized (more or less complex) cases of environmental change.

Laboratory studies have shown that trait values of phytoplankton populations change in response to variations of environmental drivers such as temperature (e.g., O'Donnell et al., 2018; Listmann et al., 2016; Padfield et al., 2016; Schaum et al., 2017) and/or pH (e.g., Scheinin et al., 2015; Schlüter et al., 2014; Tatters et al., 2013; Tong et al., 2018). Indications that observed trait value changes are indeed genetic are provided by evolutionary genetic studies (e.g. Mock et al., 2017) which show changes in replicable, heritable traits as a result of different environmental conditions. There is also evidence of adaptation to environmental changes in natural phytoplankton populations. For example, global analyses of phytoplanktonic thermal reaction norms (Thomas et al., 2012; 2016) indicate that organisms, irrespective of taxonomic differences, are adapted to local temperature conditions. Their optimum temperature varies with latitude and is related to the annual mean. In addition to this biogeographic consequence of temperature adaptation, direct observations of the adaptation process are available. The study by Irwin et al. (2015) suggests that temperature adaptation of phytoplankton has occurred in a region characterized by a gradual warming of 1 °C over 15 years. The authors find that the speed of adaptation depends on the difference between the past temperature niche and the new temperature regime. Furthermore, changes in temperature-dependent life cycle traits have been found in 2-year compared to 100-year old strains revived from phytoplankton resting stages (Hinners et al., 2017). All these studies point to a close connection between the environment and specific trait values of phytoplankton, and rapid adaptation seems to be responsible in many cases. Hence, aquatic ecosystem models

* corresponding author.
*E-mail address:* inga.hense@uni-hamburg.de (I. Hense).

https://doi.org/10.1016/j.jtbi.2019.01.041
0022-5193/

needs to account for this evolutionary process, in order to adequately represent plankton dynamics.

The adaptive response of plankton populations has been investigated in a number of modelling studies (e.g. Collins, 2016; DeLong and Gibert, 2016; Denman, 2017; Grimaud et al., 2015; Kremer and Klausmeier, 2013; Norberg et al., 2012; Sauterey et al., 2017; Shoresh et al., 2008; Smith et al., 2016). A widely used approach to account for adaptation through trait changes is based on *fitness gradients*. Several varieties of this method exist, but the underlying principle is the same (see Abrams, 2001; Abrams et al., 1993). Basically, changes in trait values are taken into account by assuming that the rate of trait value change is proportional to the rate of change in the population's *fitness* (usually its growth rate). This approach (also known as "adaptive dynamics model" or "phenotypic trait model") has been included in a number of aquatic ecosystem models (e.g. Grimaud et al., 2015; Jiang et al., 2005; Klauschies et al., 2016; Kremer and Klausmeier, 2013; 2017; Norberg et al., 2012). These model systems have been successfully applied to study, for example, the change in phytoplankton's optimum growth temperature (Grimaud et al., 2015), evolutionary changes in phytoplankton cell size (Jiang et al., 2005) or changes in edibility of phytoplankton and selectivity of zooplankton (Klauschies et al., 2016). The method is attractive because it can be included in a straightforward way in even complex ecosystem models. Yet, the approach has also well-known limitations (see, e.g. Abrams et al., 1993; Kremer and Klausmeier, 2013). In particular, applying the fitness gradient may be difficult for complex fitness landscapes which may be discontinuous and conditional, involving thresholds (e.g. for the formation of resting stages), so that fitness gradients cannot be readily prescribed. Models based on fitness gradients may thus not be flexible enough to account for all possible circumstances.

A method that explicitly accounts for the distribution of adaptive traits in a population are so-called "trait-diffusion models" (Kremer and Klausmeier, 2013; Merico et al., 2014; Sauterey et al., 2017). The "spreading of trait values" in a population as the result of mutations can be mathematically represented by a diffusion term in trait space, hence the name of this approach. So far, trait diffusion models have not been used to address evolutionary questions but rather to study aspects of plankton diversity. While Merico et al. (2014) as well as Smith et al. (2016) solve an integrated form of a trait diffusion model and focus on mean and variance of the trait value distribution, a fully discrete system of trait diffusion equations is used by Kremer and Klausmeier (2013) and Sauterey et al. (2017). Kremer and Klausmeier (2013) report little difference between their trait diffusion model and a fitness gradient based model.

A fundamentally different model approach treats the respective processes on the individual instead of the compartment level. Such *individual based models* (IBMs) have been applied in a number of eco-evolutionary studies (see Romero-Mujalli et al., 2018, for an overview). Only few of these studies focus on plankton and their trait value changes. Prominent examples are Clark et al. (2011), who consider the effect of random mutations on resource competition in an ecosystem, and Collins (2016) who addresses the growth rate response of a population to a sudden environmental change. In both cases, the distribution of trait values and its temporal evolution are not further examined.

In this study, we investigate the trait value changes in a phytoplankton population in response to environmental changes, in this case temperature. We use two fundamentally different approaches to deal with mutation and selection, one based on individuals (MuSe-IBM) the other based on multiple compartments (MuSe-MCM). Both methods are embedded in a simple ecosystem model, that allows cycling of a limiting nutrient, and are applied in a number of idealized model setups. We are interested in how well the two fundamentally different model approaches deal with a number of scenarios, including one where the fitness landscape is unclear.

**BOX 1 Definition of terms in this study.**

A **trait** is an inherited characteristic of a species (e.g., a general temperature dependence of growth). Specific (continuous or discrete) **trait values** determine the actual variant of the trait in an organism (e.g., the functional dependency including an optimum temperature and width of the thermal reaction norm).

**Adaptation** is the *heritable* adjustment of trait values within a species, leading to a fitness increase. Adaptation is caused by mutation and subsequent intraspecific (and possibly interspecific) selection, often as a response to environmental changes.

A **Multi Compartment Model** is a mathematical model to describe the way material is partitioned between compartments in a system. Each compartment represents a homogeneous, uniform collection (or collective) of entities (molecules, cells). Compartments are connected by fluxes between them, which represent processes like uptake/growth, mortality, and remineralization. The quantity in a compartment is usually given as a concentration of a so-called *model currency*, in mmol $m^{-3}$.

An **Individual Based Model** (also called **Agent Based Model**) is a computational model for simulating the actions (and interactions) of independent individuals in a system. They are used to investigate the collective behavior of individuals obeying simple rules in order to re-create or predict the emergence of more complex phenomena. Individual Based Models for phytoplankton use numerous individuals (each with a specific parameter set describing their traits), a heuristics for conditional branching (when to divide, how mutations will change the parameters of daughter cells), direct or indirect interaction rules and an environment (detritus and nutrient). It may include stochastic processes (e.g., for mortality) that affect individuals randomly.

## 2. Ecosystem model

The simplest form of an ecosystem with a closed element cycle in an aquatic environment is a PND model that considers three state variables: a phytoplankton population $P$ (meant to represent one specific species), a nutrient $N$ and detritus $D$. These three state variables are given by their concentration in mmol nitrogen $m^{-3}$, because nitrogen is the most limiting nutrient in marine ecosystems and a uniform model currency avoids conversion factors. Changes of these variables over time are the result of source and sink processes. The system of equation reads:

$$\frac{dP}{dt} = \mu(N,T)P - \gamma_o P \tag{1}$$

$$\frac{dN}{dt} = -\mu(N,T)P + \tau_o D \tag{2}$$

$$\frac{dD}{dt} = \gamma_o P - \tau_o D \tag{3}$$

where $\mu$ is the actual growth rate (dependent on resource availability and temperature); $\gamma_o$ denotes the phytoplankton mortality and $\tau_o$ the remineralization rate. These equations can be integrated numerically; for example, using the simple Euler Forward Scheme leads to the following equations:

$$P^{n+1} = P^n + \Delta t\,\mu(N,T)P^n - \Delta t\,\gamma_o P^n \tag{4}$$

$$N^{n+1} = N^n - \Delta t \mu(N,T) P^n + \Delta t \tau_o D^n \tag{5}$$

$$D^{n+1} = D^n - \Delta t \gamma_o P^n - \Delta t \tau_o D^n \tag{6}$$

where $n$ and $n+1$ are the time levels, and $\Delta t$ is the time step. Other, higher order integration schemes (such as Runge-Kutta) may be used instead.

In this set of coupled equations, the growth rate $\mu$ is the product of three terms:

$$\mu = \mu_o \times \mathcal{F}_T(T) \times \mathcal{F}_N(N). \tag{7}$$

where $\mu_o$ is the maximum (exponential) growth rate while $\mathcal{F}_T(T)$ and $\mathcal{F}_N(N)$ are the limitation terms for temperature and nutrient, respectively.

For our standard case we assume that the temperature dependence is a symmetric Gaussian (so that our solutions have an element of symmetry and any deviation from that symmetry would indicate an inaccuracy):

$$\mathcal{F}_T(T) = \exp\left[-\left(\frac{T - T_{opt}}{\theta}\right)^2\right] \tag{8}$$

where $T_{opt}$ is the optimum temperature and $\theta$ is a measure of the width of the thermal reaction norm. Nutrient limitation is represented by a Michaelis-Menten function:

$$\mathcal{F}_N(N) = \frac{N}{k_N + N} \tag{9}$$

where $k_N$ is the half-saturation constant. For simplicity, light limitation and hence self-shading effects are not considered.

## 3. Individual based model (MuSe-IBM)

### 3.1. Model concept

As mutations occur on the level of the individual, the most natural and obvious approach is to treat the phytoplankton population as a collective of individuals. Hence, we replace the phytoplankton compartment of the ecosystem model by a collective of individual cells. In our case, they are represented by their biomass $b_i$ (affected by growth and mortality) and their optimum temperature $T_{opt}$ (affected by mutation).

Several individual based models are available in the marine ecosystem modelling community (e.g., Hellweger et al., 2008; Woods, 2005); we adopt the concept from the individual based diatom life cycle model by Hense and Beckmann (2015). Individual cells grow according to

$$\frac{db_i}{dt} = \mu_i \tag{10}$$

where the doubling rate $\mu_i$ (in units mmol N $d^{-1}$) is dependent on temperature $T$, and limited by the nutrient $N$,

$$\mu_i = \mu_o / \ln 2 \times b_o \times \mathcal{F}_T(T, T_{opt}) \times \mathcal{F}_N(N) \tag{11}$$

where $\mu_o/\ln(2)$ is the maximum doubling rate and $b_o$ is the minimum (or reference) biomass (in mmol N). Each cell grows until its biomass is equal or larger than the maximum biomass $2b_o$. The cell then divides, increasing the number of live cells by one, each receiving half the biomass of the parent cell. This way, the total living biomass is conserved. The concentration of the phytoplankton population is then obtained diagnostically from

$$P = \frac{1}{V}\sum_{i=1}^{M} b_i \tag{12}$$

where $M$ is the number of live cells in the model and $V$ is the volume of the domain under consideration.

Mortality in an IBM is a stochastic process. A cell is assumed to die, if

$$\mathcal{X}_{(0,1)} < \gamma^{crit} \tag{13}$$

where $\mathcal{X}_{(0,1)}$ is sampled at each time step from the uniform distribution $\mathcal{U}(0,1)$ and the "mortality threshold" is

$$\gamma^{crit} = \gamma_o \Delta t \tag{14}$$

a non-dimensional number, combining the mortality rate $\gamma_o$ and the time step $\Delta t$. Note the conceptual requirement that $\gamma_o \leq \Delta t^{-1}$, i.e., that the loss process is resolved by the time integration scheme.

The number of live cells in the model then varies according to the cell division and mortality conditions. The corresponding discrete equation reads:

$$\frac{\Delta M}{\Delta t} = \frac{\text{number of cell divisions - number of deaths}}{\Delta t} \tag{15}$$

where

$$\text{number of cell divisions} = \sum_{i=1}^{M} \begin{cases} 1 & \text{if} \quad b_i \geq 2b_o \\ 0 & \text{else} \end{cases} \tag{16}$$

$$\text{number of deaths} = \sum_{i=1}^{M} \begin{cases} 1 & \text{if} \quad \mathcal{X}_{(0,1)} \leq \gamma^{crit} \\ 0 & \text{else} \end{cases} \tag{17}$$

While phytoplankton is treated as a collective of individuals (and replaces Eq. 1), nutrient $N$ and detritus $D$ are represented as compartments (see Eqs. 2 and 3). For the coupling, the individual based nutrient uptake as a sink to the nutrient compartment sums all the individual growth terms of the current time step

$$\mu P = \frac{1}{V}\sum_{i=1}^{M} \mu_i \tag{18}$$

while individual based phytoplankton mortality is coupled to the detritus compartment $D$ by collecting the biomass from all cells that died during the time step:

$$\gamma_o P = \frac{1}{V \Delta t}\sum_{i=1}^{M} \begin{cases} b_i & \text{if} \quad \mathcal{X}_{(0,1)} \leq \gamma^{crit} \\ 0 & \text{else} \end{cases} \tag{19}$$

The change in trait value of the cell is implemented as follows: every several hundred cell divisions one of the daughter cells experiences a *mutation* (e.g., Lenski and Travisano, 1994), in our case a change of $T_{opt}$, randomly chosen from a Gaussian distribution centered at the parent's value with a prescribed standard deviation. This way, we allow for a continuous spectrum of mutation step sizes, where small step mutations are much more likely than large step mutations. (Comments on another statistical representation of the mutation process are given in Appendix A.) Each mutation may represent an improvement or a deterioration of the competitive ability of the daughter cell. Selection through the environment will then determine which cells grow and reproduce most rapidly (see Fig. 1). The categorization of cells into "bins" ("classes" or "genotypes") is done diagnostically.

In practice, typical cell concentrations in nature prohibit the use of one model variable per cell; therefore, one model variable combines $10^4$ identical cells into one "agent" (or "supercell"). Some mutation of such an agent is assumed to take place at each division, with a smaller standard deviation $\sigma_M$. This way, part of the stochasticity of the system is eliminated, so that we do not have to use an ensemble of experiments with different sequences of random numbers to obtain a robust result. The model then tracks about $10^6$ independent agents, representing $10^{10}$ cells in

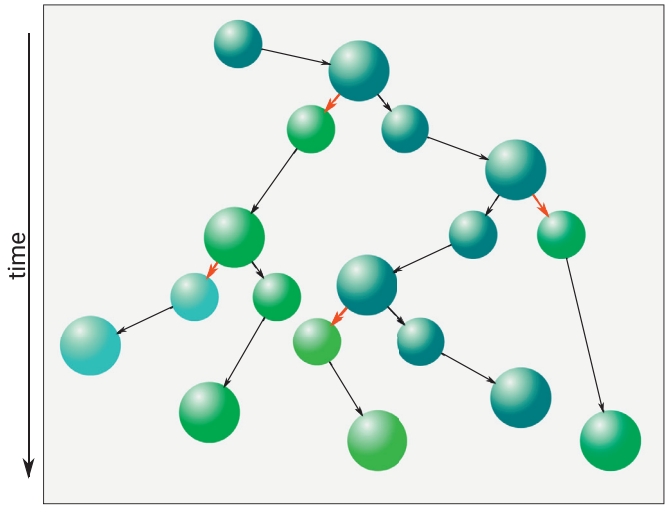


**Fig. 1.** Conceptual picture of the mutation and selection process in MuSE-IBM. After a cell has reached its maximum size, it divides; one of the daughter cells has a slightly different trait value due to mutation (indicated by the red arrow and a change in color of the cell). The resulting different growth rates lead to preferential cell division of the best adapted lineage, leading to their dominance. (For interpretation of the references to colour in this figure legend, the reader is referred to the web version of this article.)

total. During the course of the simulation, the number of active agents changes (due to cell division and mortality). In some individual based models (see, e.g. Clark et al., 2011; Woods, 2005) the number of agents (and the computational effort) is kept approximately constant by adjusting the number of cells per agent by splitting or merging. Here, we do not use such a technique, as the latter would lead to averaged cell properties (biomass, $T_{opt}$), which would distort the results. Instead, we minimize artificial statistical effects by using a very large number of agents (the dependence of results on the resolution is discussed in Appendix B).

### 3.2. Configuration

The model configuration is a well-mixed (zero-dimensional) "tank" without external sources and sinks of phytoplankton (immigration, emigration), nutrients and detritus (addition and removal). This set-up has the advantage of a closed mass balance at all times (unlike semi-continuous cultures or a chemostat, in which the total mass varies with actual phytoplankton growth rate and depends on another parameter, the dilution rate). Our general model approach, however, is independent of the specific configuration and may also be used to simulate chemostats and other laboratory configurations that exclude the mortality-remineralization-growth feedback.

The phytoplankton population is initialized by randomly assigning the biomass of each agent (distributed uniformly between minimum $b_o$ and maximum $2b_o$ biomass). This way, the initial population starts with overlapping generations. The trait values $T_{opt}$ in the population are either initialized uniformly distributed between 5 and 25 °C, or normally distributed (centered at 15 °C) with a specific standard deviation $s$.

The model is run for several (typically 5 or 10) years (about 50–60 generations per year). For simplicity, each year consists of 12 months of 30 days each; the time step $\Delta t$ is set to one hour. All model parameters are listed in Table 1.

### 3.3. Model experiments

To illustrate model performance, we carried out a number of model experiments.

**Table 1**
Parameters for the model versions and experiments.

| model parameter | symbol | value | unit |
|---|---|---|---|
| general | | | |
| total mass concentration | R | 5 | mmol N $m^{-3}$ |
| nutrient half saturation | $k_N$ | 0.15 | mmol N $m^{-3}$ |
| maximum doubling rate | $\mu_o/\ln(2)$ | 1 | doubl. $day^{-1}$ |
| mortality rate | $\gamma_o$ | 0.1 | $day^{-1}$ |
| remineralization rate | $\tau$ | 0.25 | $day^{-1}$ |
| optimal temperature | $T_{opt}$ | variable | °C |
| scale for thermal reaction norm | $\theta$ | 6 | °C |
| time step | $\Delta t$ | 3600 | s |
| individual based model | | | |
| volume of the tank | V | 1 | $m^3$ |
| reference biomass | $b_o$ | $5 \times 10^{-10}$ | mmol N |
| standard deviation of mutations | $\sigma_M$ | 0.1 | °C |
| multi-compartment model | | | |
| max. exponential growth rate | $\mu_o$ | $\ln(2)$ | $day^{-1}$ |
| temperature width of genotypes | $\Delta T_{opt}$ | 0.1 | °C |
| genotype transfer factor | $\delta$ | 1/3 | – |
| sensitivity experiments | | | |
| scale for reaction norm asymmetry | $\Delta\theta$ | 4 | °C |
| amplitude for increasing $\mu_{\max}$ | $\mu_E$ | 0.59 | doubl. $day^{-1}$ |
| scale for increasing $\mu_{\max}$ | $\Theta$ | 15.8 | °C |
| threshold for resting phase | $\mathcal{F}_{T_{crit}}$ | 0.2 | – |
| resting stage growth | $\mu_{rest}$ | 0.01 | $day^{-1}$ |
| resting stage mortality | $\gamma_{rest}$ | 0.01 | $day^{-1}$ |

#### 3.3.1. Constant temperature

In the first experiment we investigate the distribution of $T_{opt}$ in a population at constant temperature of 15 °C. Without temperature changes, a steady state (denoted $P^*$, $N^*$, $D^*$) develops. This equilibrium can be determined *analytically* from

$$N^* = \frac{\gamma_o}{\mu - \gamma_o} k_N \tag{20}$$

$$P^* = \sum_{i=1}^{M} b_i = \frac{\tau_o}{\gamma_o + \tau_o}(R - N^*) \tag{21}$$

$$D^* = \frac{\gamma_o}{\gamma_o + \tau_o}(R - N^*) \tag{22}$$

where $R = P^* + N^* + D^*$ is the total amount of the cycling mass, set to 5 mmol $m^{-3}$. In equilibrium, growth exactly balances mortality; the population growth rate is 0.1 per day (i.e., it takes on average about 7 days for a cell with $T_{opt} = T$ to divide) and the nutrient limitation factor $\mathcal{F}_N$ is 0.074. Our parameters lead to a system with equilibrium values $P^* = 3.563$ mmol $m^{-3}$, $N^* = 0.012$ mmol $m^{-3}$ and $D^* = 1.425$ mmol $m^{-3}$, which coincide with the values computed *numerically* by the IBM.

Selection alone will produce a steady state distribution with a single peak at $T_{env}$. For a model with mutation, the result is a steady state distribution of trait values where the tendencies from mutation and selection balance. Indeed, starting from an initially uniform distribution of $T_{opt}$, it takes a few months (several dozens of generations) to gradually develop into a quasi-Gaussian distribution (Fig. 2). After four years (about 200 generations), the distribution is in steady state and some lineages have reproduced 20 times more often than others, i.e., the population consists of individuals from 20 different generations. Note that the final steady state is the same if we start from an initial distribution that is not uniform but has only a single $T_{opt}$.

This equilibrium shape of the distribution function is the result of the combined effects of continuous mutation and selection due to differential growth. This emergent balance will be used as the basis for adaptation studies with temporally changing environmental temperature.

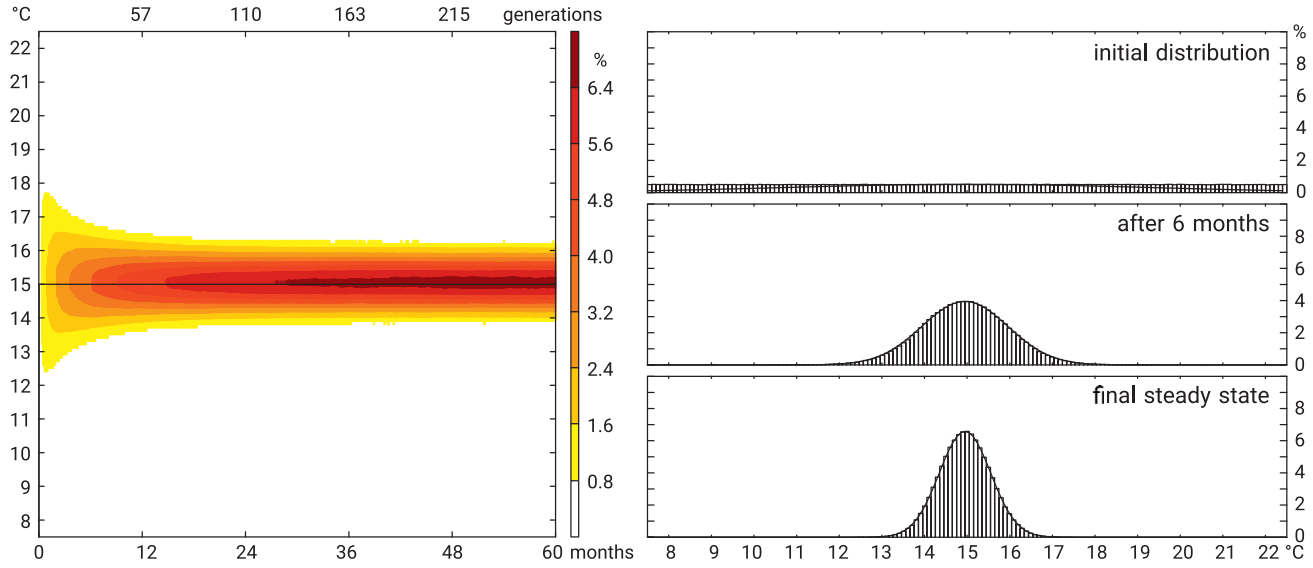


**Fig. 2.** Temporal evolution of the distribution function of $T_{opt}$ in a phytoplankton population that consists of $10^6$ individuals in a case with constant temperature at 15 °C obtained with MuSE-IBM. The left panel shows a distribution-evolution diagram over 5 years; the black line indicates the environmental temperature. The initial distribution is uniform over the range 5 to 25 °C; after about three years, the distribution has converged to a steady state. The right panels show the distribution at three instances. The best fit Gaussian function of the steady state has a standard deviation of $s = 0.855$°C. (For interpretation of the references to colour in this figure legend, the reader is referred to the web version of this article.)

We investigated a number of parameter sensitivities for this configuration: A wider *mutation range* $\sigma_M$ (i.e., larger differences between parent and daughter cell) leads to a broader distribution function, proportional to the distribution's variance $\sigma_M^2$. Similarly, a wider temperature reaction norm also causes a broader distribution. Again, a doubling of $\theta$ leads to an increase in the variance of the Gaussian distribution by a factor of two.

### 3.3.2. Sudden change in temperature

In a second experiment, the environmental temperature is assumed to change abruptly from 15 °C to 20 °C after one year of simulation. The initial distribution of $T_{opt}$ in the phytoplankton population is assumed Gaussian, the final state of the previous experiment. As an immediate response to the warmer environment the growth of the population is more severely temperature limited, leading to slower nutrient uptake. This, however, increases the nutrient availability, so that the net growth rate of the population is almost instantaneously restored to its previous (steady state) value. As individuals with a $T_{opt}$ closer to the new environmental temperature have a larger growth rate, there is a gradual shift of the mean population $T_{opt}$ towards the new temperature (Fig. 3). For our parameters, this adaptation takes about 7–8 years (350–400 generations) before the new steady state is reached. The mean $T_{opt}$ roughly follows an exponential curve, with an adaptation time scale of about 15 months (approximately 70 generations) as the best fit. Note that the adaptation time scale increases linearly with decreasing mutation range $\sigma_M$ and tighter thermal reaction norm (i.e., smaller $\theta$).

### 3.3.3. Seasonally varying temperature

Periodic variations in $T_{env}$ may be classified relative to the adaptation time scale of the phytoplankton. If the environment changes comparatively rapidly the trait value distribution within the population hardly changes at all; conversely, if the environment changes slowly or both time scales are similar, the variations will lead to a continually adapting population. In our configuration, this is the case for a seasonal cycle in temperature: the population's mean $T_{opt}$ will never reach the extreme values of the environment; instead it just varies by about $\pm$ 1 °C; the extremes of $T_{opt}$ are reached about a quarter of the seasonal cycle (i.e., 3 months, see Fig. 4).

### 3.3.4. Configurations leading to multi-modal distributions

Under certain conditions the typical uni-modal distribution of $T_{opt}$ will be replaced by more complex shapes. In particular, two (or more) subpopulations may emerge as the result of environmental conditions or phytoplankton dynamics. Such a separation of the population may be the result of one (or a combination) of the following factors:

- high frequency, abrupt and large amplitude temperature variations,
- a small mutation range (denoting the standard deviation $\sigma_M$ of parameter changes), and/or a small width of the thermal reaction norm,
- complex phytoplankton dynamics (life cycle processes, e.g., resting stage formation),

so that adaptation cannot (or need not) track the environment. This results in evolutionary branching of the population. We have simulated this in two additional configurations.

The first one combines the first two factors: it is forced by a square wave (i.e., alternating temperature) of diurnal period with an amplitude of 5 °C to obtain a clear signal. Starting from a Gaussian initial distribution centered at 15 °C, the population needs about four years (200–220 generations) to completely split and form a bimodal distribution (see Fig. 5). Both modes have a very similar shape and equilibrate at about 1 °C off the environmental temperature values (see also Table 2). This is an example of intra-generational variation that drives a trans-generational response.

The other configuration uses seasonal forcing. Here, however, phytoplankton is allowed to enter a resting phase, if the growth rate drops below the threshold value $\mathcal{F}_{T_{crit}}$. This resting phase is characterized by even further reduced growth rate of 0.01/day and a corresponding mortality of 0.01/day. Hence, there is no net growth or decay during this phase and the cells survive indefinitely. This configuration leads to three subpopulations (see Fig. 6); one with $T_{opt}$ near the average temperature of 15 °C, and two near the extreme temperatures (at 10 and 20 °C, during winter and summer, respectively). Each subpopulation survives the

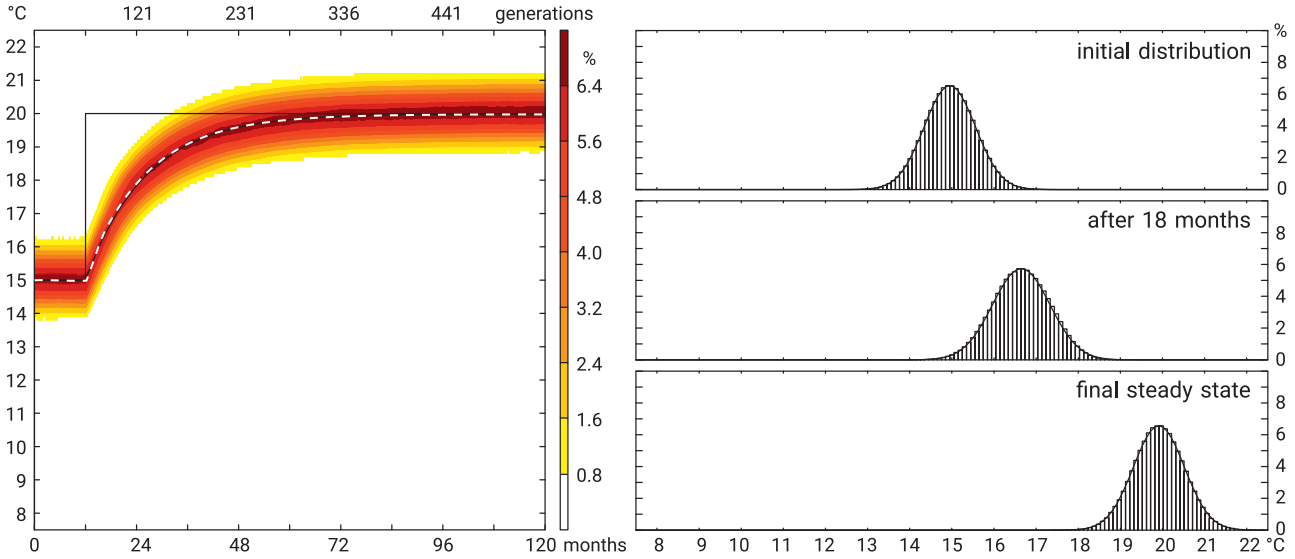


**Fig. 3.** Like Fig. 2 obtained with MuSE-IBM, but in a case where the environmental temperature changes abruptly from 15 °C to 20 °C. The left panel shows a distribution-evolution diagram over 10 years; the black line indicates the environmental temperature. The initial distribution is the steady state from the previous experiment. An exponential curve fitted to the changing $T_{opt}$ is indicated by the white dashed line. The right panels show the distribution at three instances. During the first phase of the adjustment process, the standard deviation $s = 0.968$ is slightly larger than initially and in steady state. (For interpretation of the references to colour in this figure legend, the reader is referred to the web version of this article.)

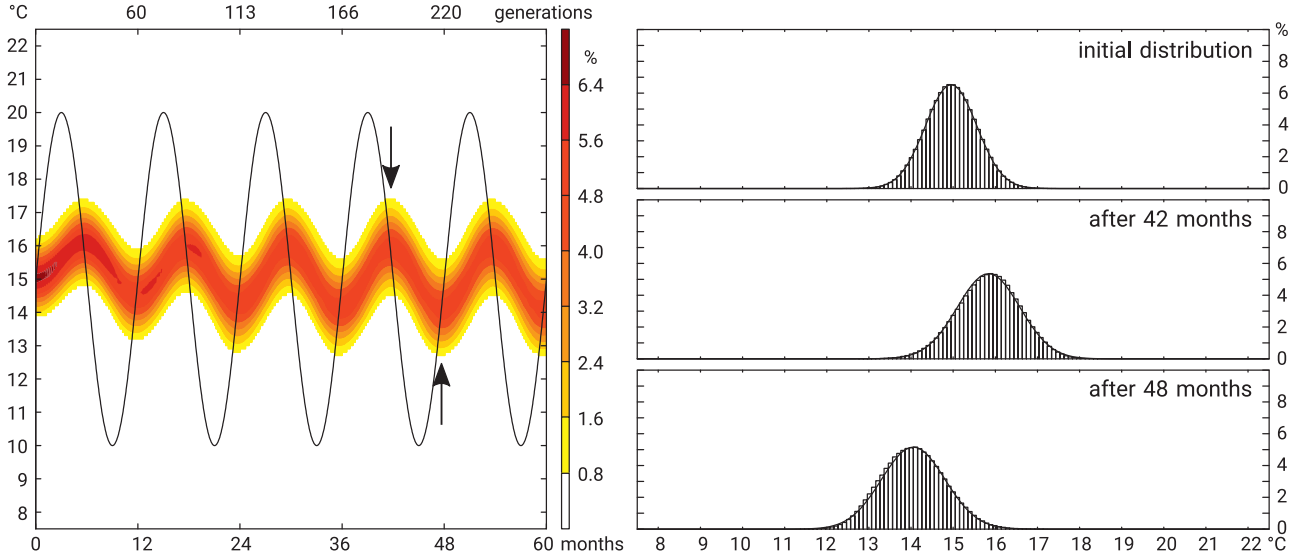


**Fig. 4.** Like Fig. 2 obtained with MuSE-IBM, but in a case where the environmental temperature changes by ±5 °C during a sinusoidal seasonal cycle. The left panel shows a distribution-evolution diagram over 5 years; the black line indicates the environmental temperature. The initial distribution is the steady state from the first experiment. The maximum of the distribution follows a sinusoidal seasonal cycle, with an amplitude that is only 20% of the environmental temperature and a time delay of about three months. The right panels show the distribution at three instances, indicating the seasonal range of $T_{opt}$ distributions. (For interpretation of the references to colour in this figure legend, the reader is referred to the web version of this article.)

unfavorable periods by resting. As a consequence, the range of co-existing generations is much wider, in our case about 120 at the end of the simulation, and still increasing. This may be ecologically important as other traits (e.g., pH dependence or toxin resistance) are also preserved in "old" cells.

### 3.3.5. Asymmetric reaction norms

In our previous experiments, we have used a symmetric temperature dependence. However, a negatively skewed thermal reaction norm for individual species is more realistic (see, e.g., Eppley, 1972; Moisan et al., 2002), i.e. the decrease is steeper for higher than for lower temperatures with distance from the optimum temperature $T_{opt}$. We use a function of the form (Hinners et al., 2017):

$$\mathcal{F}_T^*(T) = \exp\left(-\left(\frac{T - T_{opt}}{\theta + \Delta\theta\,\mathrm{sign}(T - T_{opt})}\right)^2\right) \tag{23}$$

where $\theta$ is the mean and $\Delta\theta$ the difference of the range between temperatures lower and higher than the optimum $T_{opt}$ (see Table 1).

The results are shown in Fig. 7a: carried out with constant environmental temperature $T$, we find that the population's mean $T_{opt}$ exceeds $T_{env}$, because the steeper decrease for temperatures larger than $T_{opt}$ presents a disadvantage for individuals with $T_{opt} < T_{env}$. Note that the resulting distribution function is now positively skewed.

In a second experiment the growth rate increases with temperature according to Eppley (1972). While the thermal reaction norm

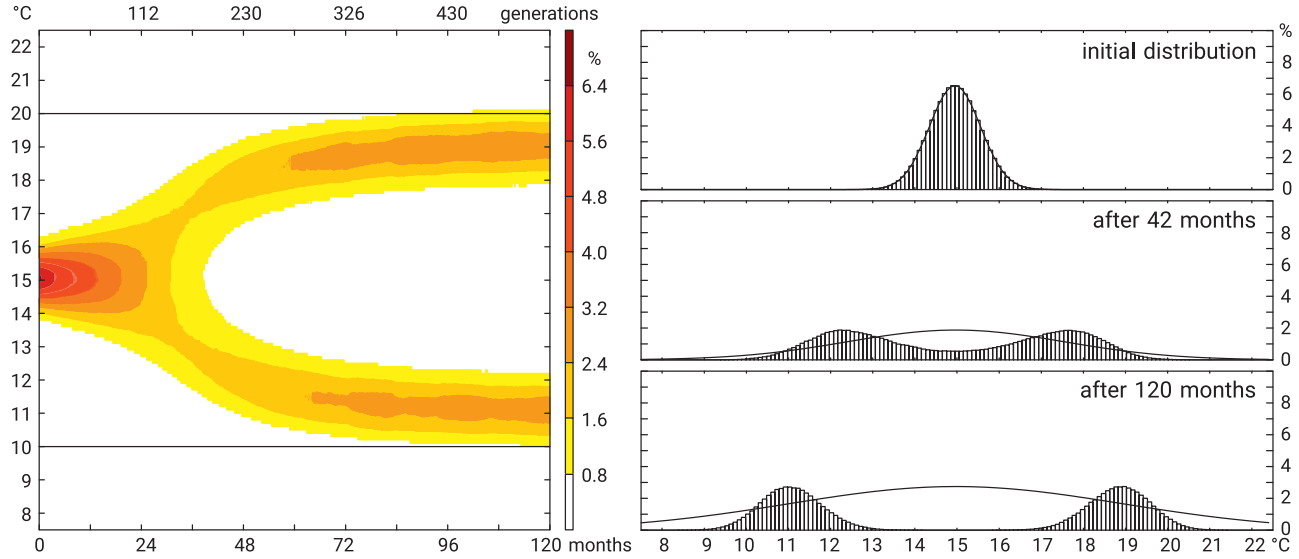


**Fig. 5.** Like Fig. 2 obtained with MuSE-IBM, but in a case where the environmental temperature changes by $\pm 5\,^{\circ}$C abruptly on a diurnal cycle. The left panel shows a distribution-evolution diagram over 10 years; the black dashed lines indicate the extreme environmental temperatures. The initial distribution is the steady state from the first experiment. The right panels show the distribution at three instances, indicating formation of two subpopulations. (For interpretation of the references to colour in this figure legend, the reader is referred to the web version of this article.)

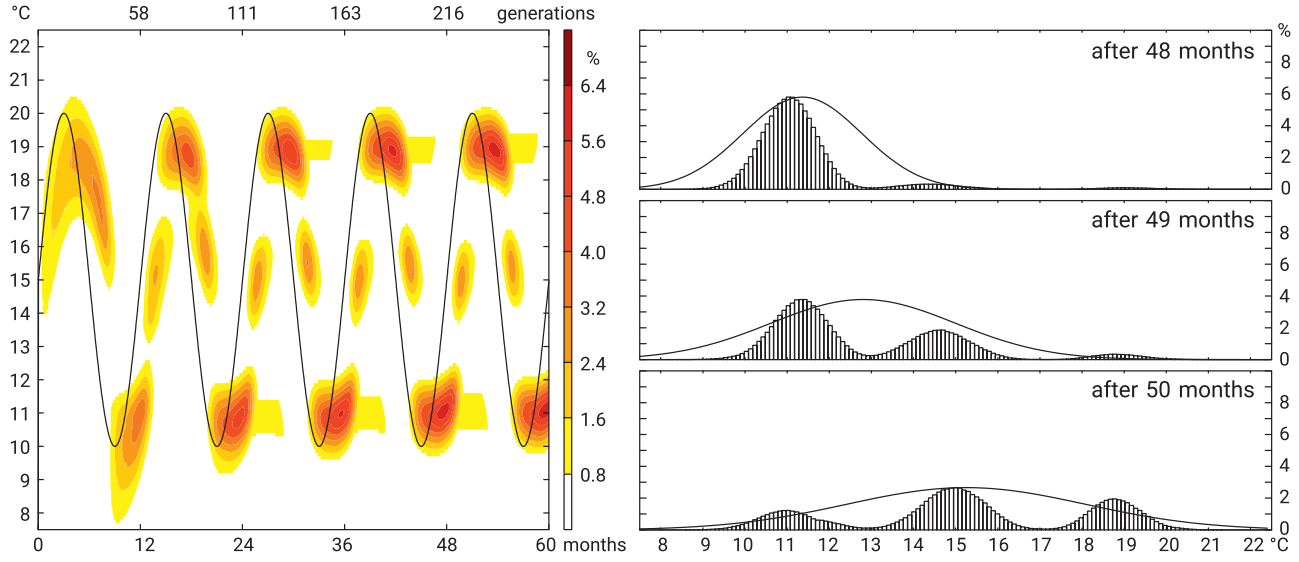


**Fig. 6.** Like Fig. 2 obtained with MuSE-IBM, but in a case where the environmental temperature changes by $\pm 5\,^{\circ}$C on a seasonal cycle. The left panel shows a distribution-evolution diagram over 5 years; the black dashed line indicates the environmental temperature. The initial distribution is a uniformly distributed $T_{opt}$. The right panels show the distribution at three instances, indicating formation of several subpopulations. (For interpretation of the references to colour in this figure legend, the reader is referred to the web version of this article.)

is Gaussian (as in our reference experiments), the maximum doubling rate $\mu_o$ (see eqn. 11) varies as

$$\mu_o = \mu_E \exp(T_{opt}/\Theta) \tag{24}$$

with $\mu_E$=0.59 doublings per day and $\Theta$=15.8 °C.

Fig. 7b shows that the population's mean $T_{opt}$ is again higher than the environmental temperature. Cells with a higher $T_{opt}$ are under positive selection, because they grow faster at higher temperature. The offset between the peak of the $T_{opt}$ distribution and the environmental temperature is related to the temperature-dependent increase in the growth rate: temperature limitation is balanced by the increase in the temperature-dependent growth rate. Cells with a $T_{opt}$ higher than the environmental temperature $T_{env}$ and thus higher growth rate perform as well as cells with a $T_{opt}$ that equals $T_{env}$ but have a lower growth rate. The location of the optimal $T_{opt}$ can be determined analytically to be

$$T_{opt} = T_{env} + \theta^2/(2\Theta) \tag{25}$$

and for the parameters used here, $T_{opt} = T_{env} + 1.14^{\circ}$C, a value that is well represented by the model.

## 4. A multi-phytoplankton-compartment model (MuSe-MCM)

### 4.1. Model concept

A compartment model version that represents the adaptive dynamics of the IBM may be constructed based on the histograms used to display the IBM's intrapopulation distribution of optimum temperature. Each of the "temperature classes" of width $\Delta T_{opt}$ may be considered a separate genotype with a specific, fixed trait value

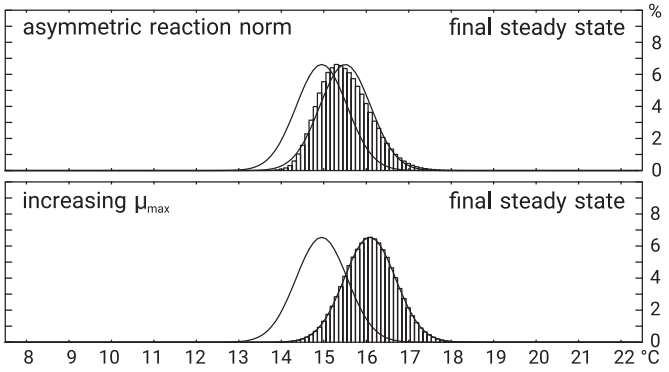


**Fig. 7.** Steady state distribution function of $T_{opt}$ in a phytoplankton population that consists of $10^6$ individuals in MuSE-IBM, with (a) an asymmetric thermal reaction norm with constant $\mu_{\max}$ but $\Delta\theta = 4^{\circ}$C, and (b) a symmetric thermal reaction norm with increasing $\mu_{\max}$. In both cases, the maximum of the distribution lies above the environmental temperature. As a reference, the distribution function for the symmetric reaction norm is also shown.

$T_{opt}$ (see Fig. 8). The concentration of each of these genotypes is then computed in a multi-compartment model.

This means we extend the ecosystem (Eqs. 1–3) to a P$^J$ND model, which leads to J+2 state variables: $J$ phytoplankton compartments $P_j$, the limiting nutrient $N$ and detritus $D$. The phytoplankton is meant to represent a specific species. The system of equations reads:

$$\frac{d\vec{P}}{dt} = \vec{\mu}\vec{P} + \mathbb{T}\vec{P} - \gamma_o\vec{P}$$

$$\frac{dN}{dt} = -\sum_{j=1}^{J}\mu_j P_j + \tau_o D$$

$$\frac{dD}{dt} = \sum_{j=1}^{J}\gamma_o P_j - \tau_o D$$

where $\vec{P} = P_j$, $(j = 1, J)$ is the vector of genotypes, $\vec{\mu} = \mu_j$, $(j = 1, J)$ is the growth vector, taking into account temperature and nutrient limitation factors ($\mathcal{F}_T$ and $\mathcal{F}_N$, respectively); as before, $\gamma_o$ denotes the mortality and $\tau_o$ the remineralization rate and $\mathbb{T}$ is the tri-diagonal growth-transfer (trait-diffusion) matrix:

$$\mathbb{T}^* = \begin{pmatrix} -\delta\mu_1 & \delta\mu_2 & 0 & 0 & \cdots & \cdots & 0 \\ \delta\mu_1 & -2\delta\mu_2 & \delta\mu_3 & 0 & \ddots & & \vdots \\ 0 & \delta\mu_2 & \ddots & \ddots & \ddots & \ddots & \vdots \\ 0 & 0 & \ddots & \ddots & \ddots & 0 & 0 \\ \vdots & \ddots & \ddots & \ddots & \ddots & \delta\mu_{J-1} & 0 \\ \vdots & & \ddots & 0 & \delta\mu_{J-2} & -2\delta\mu_{J-1} & \delta\mu_J \\ 0 & \cdots & \cdots & 0 & 0 & \delta\mu_{J-1} & -\delta\mu_J \end{pmatrix}$$

where $\delta$ is the fraction of daughter cells that belong to the neighboring genotype class (or, equivalently, the probability that mutation leads to an optimum temperature that falls into an adjacent class). Hence, the transfer rate of newly produced biomass from one to its neighboring genotype is $\mu_j\delta$, equivalent to the gradual change of properties of some of the individuals that make up the biomass of genotype $j$. For consistency, we convert the doubling rate used in the IBM to an exponential population growth rate for the compartment model (multiplication by $\ln(2)$).

The growth-transfer term $\mathbb{T}\vec{P}$ can be seen as a second order finite difference approximation to a diffusion-like term, so that the phytoplankton equation may be written as

$$\frac{\partial P}{\partial t} = \mu P + \frac{\partial^2}{\partial T_{opt}^2}\left(\mu\delta\Delta T_{opt}^2 P\right) - \gamma_o P$$

where $\mu\delta\Delta T_{opt}^2 = A_T$ represents a *mutational diffusion coefficient* in trait space. In its discrete form, the growth-transfer matrix $\mathbb{T}$ may be extended to also include an asymmetric probability of the mutations or rare large step mutations (see Appendix C).

### 4.2. Configuration

In our reference setting, we use 200 genotypes with $T_{opt}$ between 5 and 25 °C in classes of $\Delta T$ =0.1 °C (the dependence on resolution in $T_{opt}$ space is considered in the next subsection). For

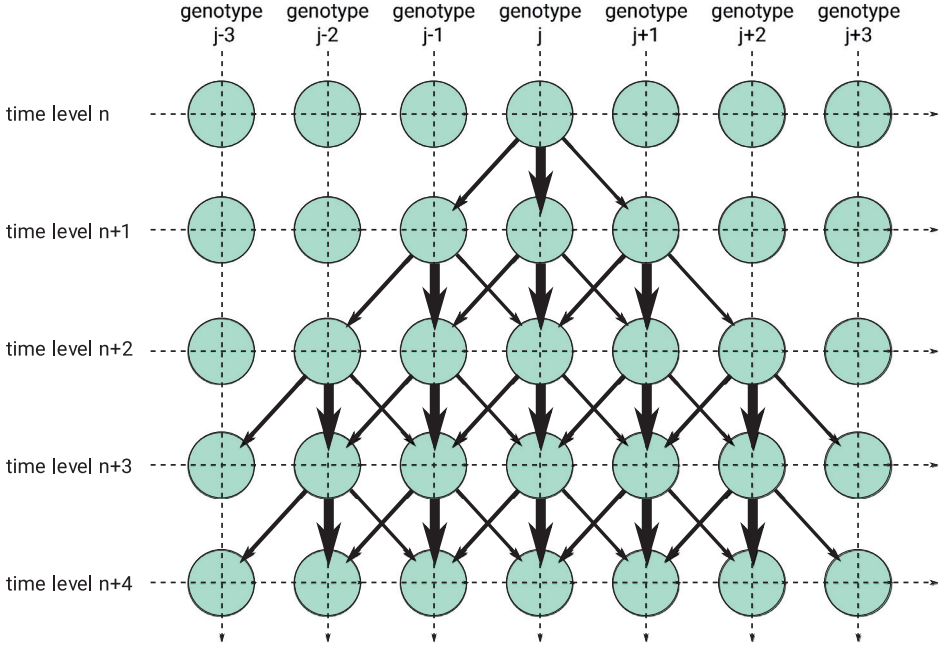


**Fig. 8.** Conceptual picture of the reallocation ("transfer") of biomass between genotypes, starting from genotype $j$, and spreading to both neighboring genotypes for MuSE-MCM. (For interpretation of the references to colour in this figure legend, the reader is referred to the web version of this article.)

**Table 2**
Statistical properties (mean and standard deviation $s$ of the $T_{opt}$ distribution) at the end of the seven experiments.

| | MuSe-IBM | | MuSe-MCM | | correlation |
|---|---|---|---|---|---|
| experiment | $\overline{T}_{opt}$ | $s$ | $\overline{T}_{opt}$ | $s$ | $R^2$ |
| constant | 15.00 | 0.859 | 15.00 | 0.855 | 0.99996 |
| sudden change | 20.00 | 0.858 | 20.00 | 0.857 | 0.99177 |
| seasonal cycle | 14.10 | 1.071 | 14.09 | 1.080 | 0.99948 |
| high frequency – full range | 15.02 | 5.636 | 14.94 | 5.626 | 0.99970 |
| – lower half | 11.09 | 1.040 | 11.09 | 1.040 | 0.99970 |
| – upper half | 18.92 | 1.039 | 18.90 | 1.038 | 0.99970 |
| asymmetric reaction norm | 15.56 | 0.854 | 15.55 | 0.833 | 0.99964 |
| exponential $\mu_o(T_{opt})$ | 16.14 | 0.861 | 16.14 | 0.857 | 0.99992 |
| seasonal resting phase | 11.43 | 2.010 | 11.43 | 1.993 | 0.99950 |

normally distributed mutations the relationship between $\delta$ and the standard deviation of the mutation range $\sigma_M$ is

$$\delta = \frac{\sigma_M^2}{3\Delta T_{opt}^2} \tag{26}$$

i.e., the transfer increases quadratically with the mutation range and decreases quadratically with the class width. Hence, we set the transfer factor $\delta$ to one third.

Although the model also runs and gives reasonable results for our configurations with $\delta > 0.5$, it is not advisable to use such large values, because the self-growth terms $(\mu_j(1-2\delta))$ of genotypes then become negative. Instead, this conceptual mismatch between mutation range and class width should be avoided by choosing a larger $\Delta T_{opt}$.

### 4.3. Model experiments

We have conducted the same seven experiments as with the IBM. In general, the compartment model solutions are very similar to the IBM results. They appear slightly smoother at times (as they are deterministic and do not suffer from the stochasticity of agents in an IBM), and are much less costly to obtain (often about two orders of magnitude). In fact, the results are so similar that no differences can be easily seen in the figures; hence, we present only a statistical comparison in Table 2. In addition to the characteristics of the distribution, the best fit adjustment time scale for the sudden change experiment is very similar (458.4 vs 465.5 days for the IBM), and the difference in best fit seasonal $T_{opt}$ amplitude for the seasonal cycle experiment is small (0.89 vs. 0.92 °C for the IBM).

### 4.4. Number of genotypes

The applicability of the multi-phytoplankton compartment model depends on the number of genotypes $J$ (and the width of the classes $\Delta T_{opt}$) that needs to be prescribed. They will directly affect the representation of details in the adaptation process and also determine the computational effort. Two-hundred genotypes, as used here, are certainly often prohibitive due to the computational costs (especially in three-dimensional models).

We have therefore investigated the dependence of the results on resolution $\Delta T_{opt}$. The outcome is shown in Fig. 9. Clearly, the level of detail decreases with fewer compartments, down to the point where the representation is no longer adequate. However, even in that case, the results are coarse but not unreasonable. Nevertheless, we recommend to use a resolution of the distribution function that still resolves the mutation range, i.e., $\Delta T_{opt} \leq \sigma_M$.

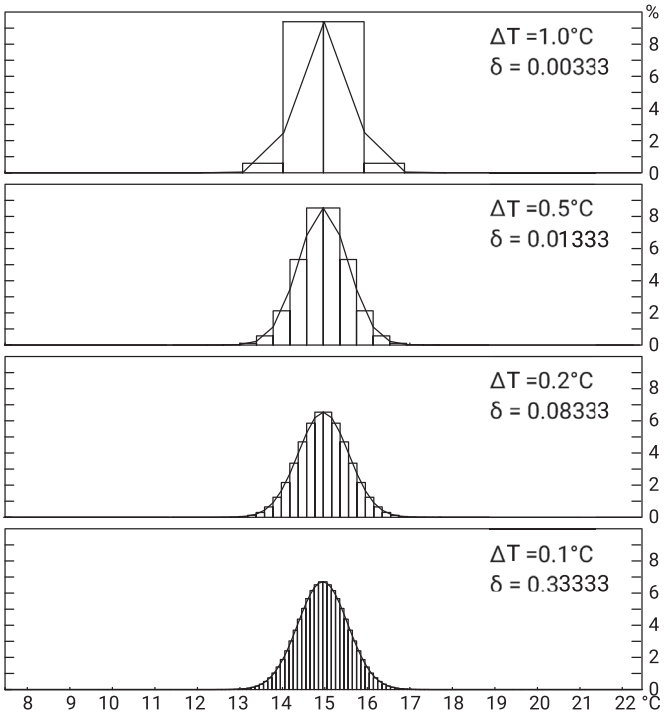


**Fig. 9.** MuSE-MCM steady state results for the constant temperature experiment, where the distribution has a standard deviation of $s = 0.855$°C (see Table 2). Note that the genotype transfer factor $\delta$ needs to be adjusted (see Eq. 26), if the number of genotypes is changed.

## 5. Summary and discussion

We have compared two different approaches to model trait value changes in unicellular asexual planktonic organisms. Both approaches are based on explicit consideration of intraspecific competition that arises from mutation and selection. The first approach, MuSe-IBM, treats phytoplankton as individuals, and introduces variation of trait values by mutation during cell division. The second approach, MuSe-MCM, considers the biomass in an array of compartments (genotypes) with prescribed trait values and allows for some transfer of biomass between genotypes during growth.

For MuSe-IBM, the controlling parameters are the number of agents and the standard deviation of mutations. Combining individuals into agents eliminates some of the stochasticity so that statistically reliable results are obtained without the need for ensemble averaging. For MuSe-MCM, the compartment width and the genotype transfer factor are decisive. We find that the standard deviation of mutations, the compartment width and the genotype transfer factor are functionally related (see Section 4.2, Eq. 26). With this relationship, and in the limit of high resolution, the results of both approaches are essentially identical.

The results of our experiments provide insight into the model performance for a suite of idealized settings. In a number of experiments both models reproduce a variety of well-known and plausible features: First, under constant environmental (temperature) conditions, a population with a trait value distribution emerges. Such a diversification in trait values has also been observed in a long-term evolutionary microbial experiment at constant conditions (Lenski and Travisano, 1994). Second, adaptation of the population to a new (constant) temperature takes a few hundred generations. This is in line with observations (e.g. Bach et al., 2018; Padfield et al., 2016; Schaum et al., 2018) showing rapid evolution of phytoplankton towards changing environmental conditions. Third, for variation on periods longer than a few dozens of

generations, the population's trait value distribution follows with smaller amplitudes and a time lag. These modes of behaviour are well known and have been described earlier (Carvalho, 1987; Ellner and Hairston, 1994; King, 1972). Fourth, the model experiment with a negatively skewed thermal reaction norm of the phytoplankton leads to an optimum growth temperature that exceeds the environmental temperature – a feature which has also been found in nature and explained by Thomas et al. (2012).

The model runs with fast (diurnal) and large environmental temperature fluctuations and those taking into account growing and resting stages result in the emergence and coexistence of separate subpopulations. This may seem surprising as the literature and canonical framework concerned with modeling evolutionary responses of microbial organisms in a changing world often ignores the possibility of the rapid formation of subpopulations (Lynch and Lande, 1993). Rather it is implied that single populations follow the changing environment through adaptive tracking when the environmental change spans many generations, though the possibility for population-level bet-hedging is hinted at as one possibility in environments that vary more rapidly (e.g. Botero et al., 2015). The assumption of there being one response that emerges as the evolutionary "winner" in a changing or changed environment stems from traditional selection experiments often being carried out in "poor quality environments" (Bell, 2012), which usually include elements of starvation (Elena et al., 1996; Lenski and Travisano, 1994), high salt stress (Bell and Gonzalez, 2011; Lachapelle and Bell, 2012), or toxicity or other depressing elements (Kawecki et al., 2012). There, a single strategy will at least initially be the best and possibly only viable strategy to survive in a changing environment. However, even under these circumstances, once populations have adapted enough to the environment to evolve beyond the minimum growth rate needed to avoid extinction, the emergence of other strategies, and thereby co-existing populations or lineages, occurs rapidly (Lenski et al., 1998; Tenaillon et al., 2016). Overall, observational, empirical, and experimental data suggest that the emergence of distinct subpopulations is far from being rare (e.g. Godhe and Rynearson, 2017; Luxem et al., 2017; Rynearson and Armbrust, 2005; Schaum et al., 2013; Wolf et al., 2018). In environments, where a change in average conditions improves or, as in our cases, does not alter the overall environmental quality, multiple equivalent strategies will allow the co-existence of more than one population. A single population with a single characteristic response of growth rates would only occur if diversity is lost through competitive exclusion, or when environmental changes are too slow to allow for population level bet-hedging.

In this study, we have focused only on one trait, optimum temperature of growth, but other (and additional) trait value changes, related for example to size, pH dependence or toxin resistance (see e.g. Barton et al., 2013; Litchman et al., 2012) may also be taken into account. Similarly, the effects of trade-offs can be implemented with relative ease in either of these two approaches. The effects of immigration and/or emigration of organisms with different trait values (see, e.g. Bruggeman and Kooijman, 2007; Kremer and Klausmeier, 2017; Sauterey et al., 2017) may be added and will be captured automatically by spatially distributed versions of our models. Overall, the advantage of MuSe-IBM and MuSe-MCM is that they are highly flexible. Both models can represent complex functional dependencies, e.g. related to the life cycle of phytoplankton, which may not easily be cast in terms of a fitness gradient. They are therefore suitable for studies in which trait value changes have unknown consequences for fitness.

We envision that MuSe-IBM will be preferred for simulations designed to represent the dynamics in laboratory configurations, while MuSe-MCM is particularly suitable for implementation in three-dimensional ecosystem models, due to its lower computational demands. Both approaches (even in combination) are useful for investigating the evolutionary path of populations and suitable to tackle a wide variety of questions in the field of planktonic evolutionary science.

## Acknowledgments

IH is supported through the Cluster of Excellence "CliSAP" (EXC177), University of Hamburg, funded through the German Science Foundation (DFG). We thank two anonymous reviewers for their positive feedback.

## Appendix A. Representation of mutation statistics

The variance of the resulting distribution is directly proportional to the range of Gaussian mutations. If we change the Gaussian distribution of mutations to one uniformly distributed over a fixed range, we also get a Gaussian distribution of the abundance of agents (as a function of $T_{opt}$). The same distribution is obtained, when the standard deviation of uniformly distributed mutations $\sigma_M$ is multiplied by $\sqrt{3}$ (as the standard deviation of a uniform distribution is $1/\sqrt{3}$). For the compartment model, the genotype transfer factor $\delta$ (see Eq. 26) is then

$$\delta = \left( \frac{\sigma_M}{\Delta T_{opt}} \right)^2 . \tag{A.1}$$

## Appendix B. Number of agents

The number of agents used in the IBM determines the statistical properties of the resulting distribution. Fig. B.10 shows the distribution functions after five years. We conclude that, $10^4$ or $10^5$ agents do not suffice, unless time- or ensemble averaging is done. All experiments in this study are carried out with $10^6$ individuals, which do not really differ from a 10 time higher resolution case.

## Appendix C. MuSe-MCM Generalizations

In this appendix, the flexibility of the MuSe-MCM approach is demonstrated using two examples.

If we have to assume that the probability of mutation depends on the direction of the trait value change (i.e., resembling advection in trait space) then the genotype transfer factor $\delta$ is no longer constant but larger in one direction than in the other. Introducing $\delta^+$ in positive and $\delta^-$ in negative direction, the growth-transfer ("trait diffusion") matrix in that case becomes

$$\mathbb{T}' = \begin{pmatrix} -\delta^+\mu_1 & \delta^+\mu_2 & 0 & 0 & \cdots & \cdots & 0 \\ \delta^-\mu_1 & -\delta^\Sigma\mu_2 & \delta^+\mu_3 & 0 & \ddots & & \vdots \\ 0 & \delta^-\mu_2 & \ddots & \ddots & \ddots & \ddots & \vdots \\ 0 & 0 & \ddots & \ddots & \ddots & 0 & 0 \\ \vdots & \ddots & \ddots & \ddots & \ddots & \delta^+\mu_{J-1} & 0 \\ \vdots & & \ddots & 0 & \delta^-\mu_{J-2} & -\delta^\Sigma\mu_{J-1} & \delta^+\mu_J \\ 0 & \cdots & \cdots & 0 & 0 & \delta^-\mu_{J-1} & -\delta^-\mu_J \end{pmatrix}$$

where $\Delta^\Sigma = \delta^+ + \delta^-$.

The growth-transfer matrix $\mathbb{T}$ may also be modified to account for occasional larger step mutations. In this case, additional matrix elements have to be set to non-zero values, for example the

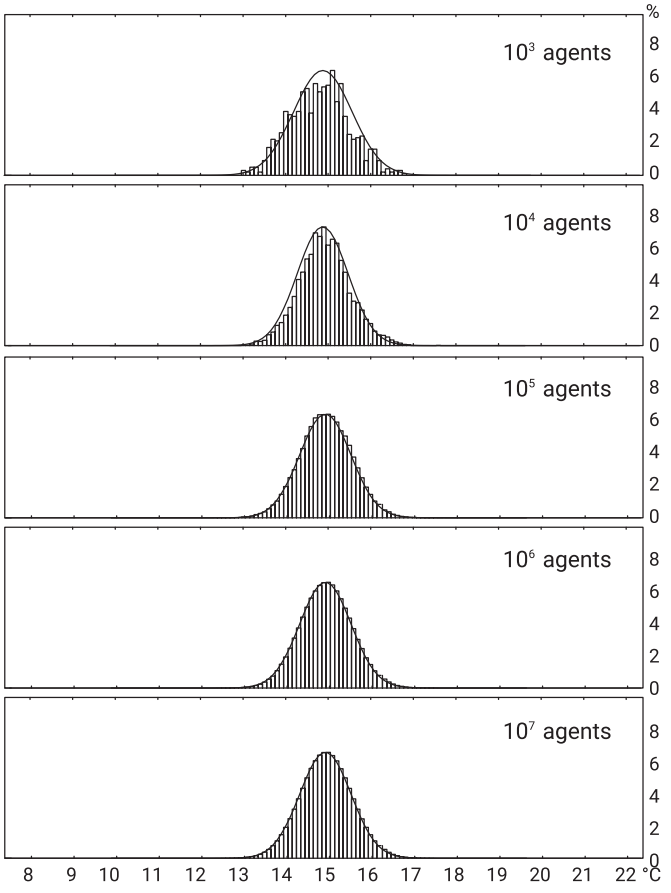


**Fig. B.10.** Quasi-steady state results for the constant temperature experiment with different number of agents. 1000 agents (each representing $10^7$ individuals) are clearly insufficient. The differences between $10^6$ and $10^7$ agents are hardly visible.

penta-diagonal matrix

$$\mathbb{T}^* = \begin{pmatrix} -\beta\mu_1 & \delta\mu_2 & \epsilon\mu_3 & 0 & \cdots & \cdots & 0 \\ \delta\mu_1 & -2\beta\mu_2 & \delta\mu_3 & \epsilon\mu_4 & \ddots & & \vdots \\ \epsilon\mu_1 & \delta\mu_2 & -2\beta\mu_3 & \ddots & \ddots & \ddots & \vdots \\ 0 & \epsilon\mu_2 & \ddots & \ddots & \ddots & \epsilon\mu_{J-1} & 0 \\ \vdots & \ddots & \ddots & \ddots & -2\beta\mu_{J-2} & \delta\mu_{J-1} & \epsilon\mu_J \\ \vdots & & \ddots & \epsilon\mu_{J-3} & \delta\mu_{J-2} & -2\beta\mu_{J-1} & \delta\mu_J \\ 0 & \cdots & \cdots & 0 & \epsilon\mu_{J-2} & \delta\mu_{J-1} & -\beta\mu_J \end{pmatrix}$$

where $\epsilon$ is the probability that a mutation leads to a $T_{opt}$ that is two genotype classes away and $\beta = (\delta + \epsilon)$.

## References


Abrams, P.A., 2001. Describing and quantifying interspecific interactions: a commentary on recent approaches. Oikos 94, 209–218.

Abrams, P.A., Harada, Y., Matsuda, H., 1993. On the relationship between quantitative genetic and ess models. Evolution 47, 982–985.

Bach, L.T., Lohbeck, K.T., Reusch, T.B.H., Riebesell, U., 2018. Rapid evolution of highly variable competitive abilities in a key phytoplankton species. Nat. Ecol. Evol. 2, 611–613.

Barton, A.D., Pershing, A.J., Litchman, E., Record, N.R., Edwards, K.F., Finkel, Z.V., Kirboe, T., Ward, B.A., 2013. The biogeography of marine plankton traits. Ecol. Lett. 16, 522–534.

Bell, G., 2012. Evolutionary rescue and the limits of adaptation. Philos. Trans. Roy. Soc. B Biol. Sci. 368, 20120080.

Bell, G., Gonzalez, A., 2011. Adaptation and evolutionary rescue in metapopulations experiencing environmental deterioration. Science 332, 1327–1330.

Botero, C., Weissing, F., Wright, J., Rubenstein, D., 2015. Evolutionary tipping points in the capacity to adapt to environmental change. Procee. Natl. Acad. Sci. 112, 184–189.

Bruggeman, J., Kooijman, S.A.L.M., 2007. A biodiversity-inspired approach to aquatic ecosystem modeling. Limnol. Oceanogr. 52, 1533–1544.

Carvalho, G.R., 1987. The clonal ecology of *Daphnia magna*(Crustacea: Cladocera): II. Thermal differentiation among seasonal clones. J. Anim. Ecol. 56, 69–478.

Clark, J., Daines, S., Lenton, T., Watson, A., Williams, H., 2011. Individual-based modelling of adaptation in marine microbial populations using genetically defined physiological parameters. Ecol. Modell. 222, 3823–3837.

Collins, S., 2016. Growth rate evolution in improved environments under Prodigal Son dynamics. Evol. Appl. 9, 1179–1188.

DeLong, J.P., Gibert, J.P., 2016. Gillespie ecoevolutionary models (gem s) reveal the role of heritable trait variation in ecoevolutionary dynamics. Ecol. Evol. 6, 935–945.

Denman, K.L., 2017. A model simulation of the adaptive evolution through mutation of the coccolithophore *Emilianiahuxleyi* based on a published laboratory study. Front. Mar. Sci. 3 (286).

O'Donnell, D.R., Hamman, C.R., Johnson, E.C., Kremer, C.T., Klausmeier, C.A., Litchman, E., 2018. Rapid thermal adaptation in a marine diatom reveals constraints and tradeoffs. Glob. Chang. Biol. https://doi.org/10.1111/gcb.14360.

Elena, S.F., Cooper, V.S., Lenski, R.E., 1996. Punctuated evolution caused by selection of rare beneficial mutations. Science 272, 1802–1804.

Ellner, S., Hairston, N.G., 1994. Role of overlapping generations in maintaining genetic variation in a fluctuating environment. Am. Nat. 14, 403–417.

Eppley, R.W., 1972. Temperature and phytoplankton growth in the sea. Fish. Bull. 70, 1063–1085.

Godhe, A., Rynearson, T., 2017. The role of intraspecific variation in the ecological and evolutionary success of diatoms in changing environments. Philos. Trans. Roy. Soc. B Biol. Sci. 372, 20160399.

Grimaud, G.M., LeGuennec, V., Ayata, S.D., Mairet, F., Sciandra, A., Bernard, O., 2015. Modelling the effect of temperature on phytoplankton growth across the global ocean. IFAC-PapersOnLine 48, 228–233.

Hairston, N.G., Ellner, S.P., Geber, M.A., Yoshido, T., Fox, J.A., 2005. Rapid evolution and the convergence of ecological and evolutionary time scales. Ecol. Lett. 8, 1114–1127.

Hellweger, F.L., Kravchuk, E.S., Novotny, V., Gladyshev, M.I., 2008. Agent-based modeling of the complex life cycle of a cyanobacterium (*Anabaena*) in a shallow reservoir. Limnol. Oceanogr. 53, 1227–1241.

Hense, I., Beckmann, A., 2015. A theoretical investigation of the diatom cell size reduction–restitution cycle. Ecol. Modell. 317, 66–82.

Hinners, J., Kremp, A., Hense, I., 2017. Evolution in temperature-dependent phytoplankton traits revealed from a sediment archive: do reaction norms tell the whole story? Procee. Roy. Soc. B 284, 1471–2954.

Irwin, A.J., Finkel, Z.V., Müller-Karger, F.E., Ghinaglia, L.T., 2015. Phytoplankton adapt to changing ocean environments. Proc. Natl. Acad. Sci. U.S.A. 112, 5762–5766.

Jiang, L., Schofield, O.M., Falkowski, P.G., 2005. Adaptive evolution of phytoplankton cell size. Am. Nat. 166, 496–505.

Kawecki, T., Lenski, R., Ebert, D., Hollis, B., Olivieri, I., Whitlock, M., 2012. Experimental evolution. Trend. Ecol. Evol. 27, 547–560.

King, C.E., 1972. Adaptation of rotifers to seasonal variation. Ecology 53, 408–418.

Klauschies, T., Vasseur, D., Gaedke, U., 2016. Trait adaptation promotes species coexistence in diverse predator and prey communities. Ecol. Evol. 6, 4141–4159.

Kremer, C.T., Klausmeier, C., 2013. Coexistence in a variable environment: eco-evolutionary perspectives. J. Theor. Biol. 339, 14–25.

Kremer, C.T., Klausmeier, C.A., 2017. Species packing in ecoâvolutionary models of seasonally fluctuating environments. Ecol. Lett. 20, 1158–1168.

Lachapelle, J., Bell, G., 2012. Evolutionary rescue of sexual and asexual populations in a deteriorating environment. Evolution 66, 3508–3518.

Lenski, R., Mongold, J., Sniegowski, P., Travisano, M., Vasi, F., Gerrish, P., Schmidt, T., 1998. Evolution of competitive fitness in experimental populations of *E. coli*: what makes one genotype a better competitor than another? Antonie Van Leeuwenhoek 73, 35–47.

Lenski, R., Travisano, M., 1994. Dynamics of adaptation and diversification: a 10,000-generation experiment with bacterial populations. Procee. Natl. Acad. Sci. 91, 6808–6814.

Listmann, L., LeRoch, M., Schlüter, L., Thomas, M.K., Reusch, T.B., 2016. Swift thermal reaction norm evolution in a key marine phytoplankton species. Evol. Appl. 9, 1156–1164.

Litchman, E., Edwards, K.F., Klausmeier, C.A., Thomas, M.K., 2012. Phytoplankton niches, traits and eco-evolutionary responses to global environmental change. Mar. Ecol. Prog. Ser. 470, 235–248.

Lohbeck, K., Riebesell, U., Reusch, T.B.H., 2012. Adaptive evolution of a key phytoplankton species to ocean acidification. Nat. Geosci. 5, 346–351.

Luxem, K.E., Ellwood, M.J., Strzepek, R.F., 2017. Intraspecific variability in *Phaeocystis Antarctica*'s response to iron and light stress. PLoS ONE 12, e0179751.

Lynch, M., Lande, R., 1993. Evolution and extinction in response to environmental change. In: Kareiva, P.M., Kingsolver, J.G., Huey, R.B. (Eds.), Biotic interactions and global change. Sinaller Associates, Sunderland, MA (USA), p. 571.

Merico, A., Brandt, G., Smith, S., Oliver, M., 2014. Sustaining diversity in trait-based models of phytoplankton communities. Front. Ecol. Evol. 2, 59.

Mock, T., Otillar, R.P., Strauss, J., McMullan, M., Paajanen, P., Schmutz, J., Salamov, A., Sanges, R., Toseland, A., Ward, B.J., Allen, A.E., Dupont, C.L., Frickenhaus, S., Maumus, F., Veluchamy, A., Wu, T., Barry, K.W., Falciatore, A., Ferrante, M.I., Fortunato, A.E., Glöckner, G., Gruber, A., Hipkin, R., Janech, M.G., Kroth, P.G., Leese, F., Lindquist, E.A., Lyon, B.R., Martin, J., Mayer, C., Parker, M., Quesneville, H., Ray-

mond, J.A., Uhlig, C., Valasand, R.E., Valentin, K.U., Worden, A.Z., Armbrust, E.V., Clark, M.D., Bowler, C., Green, B.R., Moulton, V., Oosterhout, C.V., Grigoriev, I., 2017. Evolutionary genomics of the cold-adapted diatom *Fragilariopsis cylindrus*. Nature 541, 536–540.

Moisan, J., Moisan, T., Abbott, M., 2002. Modelling the effect of temperature on the maximum growth rates of phytoplankton populations. Ecol. Modell. 153, 197–215.

Romero-Mujalli, D., Jeltsch, F., Tiedemann, R., 2018. Individual-based modeling of eco-evolutionary dynamics: state of the art and future directions. Reg. Environ. Change 1–12. https://doi.org/10.1007/s10113-018-1406-7.

Norberg, J., Urban, M.C., Vellend, M., Klausmeier, C.A., Loeuille, N., 2012. Eco-evolutionary responses of biodiversity to climate change. Nat. Clim. Chang. 2, 747–751.

Padfield, D., Yvon-Durocher, G., Buckling, A., Jennings, S., Yvon-Durocher, G., 2016. Rapid evolution of metabolic traits explains thermal adaptation in phytoplankton. Ecol. Lett. 19, 133–142.

Rynearson, T.A., Armbrust, E.V., 2005. Maintenance of clonal diversity during a spring bloom of the centric diatom *ditylumbrightwellii*. Mol. Ecol. 14, 1631–1640.

Sauterey, B., Ward, B., Rault, J., Bowler, C., Claessen, D., 2017. The implications of eco-evolutionary processes for the emergence of marine plankton community biogeography. Am. Nat. 190, 116–130.

Schaum, C., Barton, S., Bestion, E., Buckling, A., Garcia-Carreras, B., Lopez, P., Lowe, C., Pawar, S., Smirnoff, N., Trimmer, M., Yvon-Durocher, G., 2017. Adaptation of phytoplankton to a decade of experimental warming linked to increased photosynthesis. Nat. Ecol. Evol. 1 (0094).

Schaum, C., Buckling, A., Smirnoff, N., Studholme, D., Yvon-Durocher, G., 2018. Environmental fluctuations accelerate molecular evolution of thermal tolerance in a marine diatom. Nat. Commun. 9 (1719).

Schaum, E., Rost, B., Millar, A.J., Collins, S., 2013. Variation in plastic responses of a globally distributed picoplankton species to ocean acidification. Nat. Clim. Chang. 3, 298–302.

Scheinin, M., Riebesell, U., Rynearson, T.A., Lohbeck, K.T., Collins, S., 2015. Experimental evolution gone wild. Journal of The Royal Society Interface 12, 20150056.

Schlüter, L., Lohbeck, K.T., Gutowska, M.A., Gröger, J.P., Riebesell, U., Reusch, T.B., 2014. Adaptation of a globally important coccolithophore to ocean warming and acidification. Nat. Clim. Chang. 4, 1024–1030.

Shoresh, N., Hegreness, M., Kishony, R., 2008. Evolution exacerbates the paradox of the plankton. Procee. Natl. Acad. Sci. 105, 12365–12369.

Smith, S.L., Vallina, S.M., Merico, A., 2016. Phytoplankton size-diversity mediates an emergent trade-off in ecosystem functioning for rare versus frequent disturbances. Sci. Rep. 6, 34170.

Tatters, A.O., Roleda, M.Y., Schnetzer, A., Fu, F., Hurd, C.L., Boyd, P.W., Caron, D.A., Lie, A.A.Y., Hoffmann, L.J., Hutchins, D.A., 2013. Short- and long-term conditioning of a temperate marine diatom community to acidification and warming. Philos. Trans. Roy. Soc. B 368, 20120437.

Tenaillon, O., Barrick, J., Ribeck, N., Deatherage, D., Blanchard, J., Dasgupta, A., Wu, G., Wielgoss, S., Cruveiller, S., Médigue, C., Schneider, D., 2016. Tempo and mode of genome evolution in a 50,000-generation experiment. Nature 536, 165–170.

Thomas, M.K., Kremer, C.T., Klausmeier, C.A., Litchman, E., 2012. A global pattern of thermal adaptation in marine phytoplankton. Science 338, 1085–1088.

Thomas, M.K., Kremer, C.T., Litchman, E., 2016. Environment and evolutionary history determine the global biogeography of phytoplankton temperature traits. Global Ecol. Biogeogr. 25, 75–86.

Tong, S., Gao, K., Hutchins, D.A., 2018. Adaptive evolution in the coccolithophore gephyrocapsa oceanica following 1,000 generations of selection under elevated co2. Glob. Chang. Biol. 24, 3055–3064.

Wolf, K.K.E., Hoppe, C.J.M., Rost, B., 2018. Resilience by diversity: large intraspecific differences in climate change responses of an arctic diatom. Limnol. Oceanogr. 63, 397–411.

Woods, J.D., 2005. The Lagrangian ensemble metamodel for simulating plankton ecosystems. Prog. Oceanogr. 67, 84–159.